Applied Physics Letters

# Coherent control of transverse modes in semiconductor laser frequency combs via radio-frequency injection

Cite as: Appl. Phys. Lett. **121**, 071106 (2022); https://doi.org/10.1063/5.0098474
Submitted: 09 May 2022 • Accepted: 22 July 2022 • Published Online: 17 August 2022

Sandro Dal Cin, Florian Pilat, Aleš Konečný, et al.







AIP Publishing

Applied Physics Letters ARTICLE scitation.org/journal/apl

# Coherent control of transverse modes in semiconductor laser frequency combs via radio-frequency injection

Cite as: Appl. Phys. Lett. **121**, 071106 (2022); doi: 10.1063/5.0098474
Submitted: 9 May 2022 · Accepted: 22 July 2022 ·
Published Online: 17 August 2022



Sandro Dal Cin,[1,a)] Florian Pilat,[1] Aleš Konečný,[1] Nikola Opačak,[1] Gottfried Strasser,[1,2] and Benedikt Schwarz[1]

## AFFILIATIONS

[1]Institute of Solid State Electronics, TU Wien, Gusshausstrasse 25-25a, 1040 Vienna, Austria
[2]Zentrum für Mikro- und Nanostrukturen, TU Wien, Gusshausstrasse 25-25a, 1040 Vienna, Austria

[a)]Author to whom correspondence should be addressed: sandro.cin@tuwien.ac.at

## ABSTRACT

Increasing the output power of semiconductor laser frequency combs, while maintaining a single-lobe far-field characteristic is of great interest for mid-infrared sensing applications. Broadening of the ridge waveguide represents the most common approach for power scaling, however, the excitement of higher-order transverse modes often limits general applicability. Here, we demonstrate that the coherent control of the longitudinal laser modes enables control over the transverse modes of a quantum cascade laser. Modulating the laser in a frequency range $60 \pm 3$ MHz above the free-running laser beatnote and applying modulation powers above 25 dBm provides reliable fundamental transverse mode operation, observable as single-lobe, Gaussian-like characteristic in the recorded far-field. Furthermore, coherent comb operation for both fundamental and higher-order transverse mode states is demonstrated.



The quantum cascade laser (QCL) has been established in a diverse range of novel spectroscopy, sensing, and diagnostics applications as a reliable and compact source of coherent mid-infrared (MIR) and terahertz light.[1–4] Furthermore, QCLs possess a large resonant optical non-linearity, which facilitates the spontaneous formation of free-running optical frequency combs,[5] rendering QCLs appealing as broadband frequency rulers for metrology and spectroscopy.[6,7] A more refined insight into MIR frequency comb formation mechanisms has led to novel findings and advances in the field, including self-starting harmonic frequency combs,[8] frequency combs triggered by phase turbulence,[9] and the emission of dissipative Kerr solitons.[10] The ability to control and produce this wide variety of states on demand is of utmost importance for potential applications. Radio-frequency (RF) modulation of the laser driving current was proven to be of great use to achieve this. Coherent RF injection locking of the laser repetition frequency has enabled stable and robust Fabry–Pérot (FP) combs,[11] switching between frequency-modulated (FM) and amplitude-modulated (AM) synchronization states,[12] active mode locking, the emission of pulses,[13–15] and significant spectral broadening.[16,17] Based on the manifold possibilities for tailoring of comb states in FP-QCLs employing RF-modulation, the findings presented in this article can further enhance the quality of comb operation in terms of performance and most notably in combination with mode locking and spectral broadening under high power RF-injection.

High performance and high output power remain one of the main driving forces behind QCL development, and output powers up to several Watt per facet have already been demonstrated.[18–20] Besides implementing laser arrays,[21–23] one way to achieve this is by increasing the QCLs ridge width. While combination of individual narrow ridge QCLs can provide similar performance in terms of power, it is significantly harder to achieve a frequency comb output for such configurations. In comparison, increasing the ridge width of a FP-QCL enables power scaling, while still providing the possibility for coherent comb operation. However, broad ridges often lead to the excitement of higher-order transverse modes, manifested as two or more separated intensity lobes with minima in between that can be observed in their far-field characteristic.[24] This behavior is known to be undesirable for many applications where a single-lobe fundamental mode is favored.[25–27] In this work, we investigate the impact of RF-modulation on transverse cavity mode switching in a 12 $\mu$m wide ridge waveguide

FP-QCL. In order to gain more insight into the supported transverse cavity modes, we utilize a custom two-dimensional cavity mode solver tool. The wet-etched QCL waveguide passivated using MOCVD InP regrowth is implemented into the mode solver tool including the corresponding frequency-dependent effective refractive indices of the QCL structure. The QCL ridge waveguide outlines are shown in Figs. 1(a) and 1(c), superimposed with the simulation results of the supported transverse mode profiles in the active region (AR). The simulations indicate that the modeled cavity supports at least two transverse modes. Most importantly here are the fundamental mode with a single-lobe, and a second-order mode comprised of two lobes with an intensity minimum in between. This is shown in Figs. 1(a)–1(c). The repetition frequency $f_{\mathrm{rep}}$, which is equal to the free spectral range of the FP cavity, is calculated using the group refractive index given by $n_g(\nu) = n_{eff}(\nu) + \nu \frac{dn_{eff}(\nu)}{d\nu}$. Here, $n_{eff}$ is the effective refractive index of a simulated transverse mode and $\nu$ is the optical frequency. By utilizing the calculated mode-specific $n_g$, we find that the $f_{rep}$ of the fundamental mode is located several MHz above the $f_{rep}$ of the second-order mode in the free-running laser as illustrated in Fig. 1(d). The numerical values of $f_{rep}$ and $n_g$ obtained from the mode solver tool are shown in Figs. 1(a) and 1(c).

For any laser that emits a coherent frequency comb, all evenly spaced modes in the optical domain beat together and create a beating at the difference frequency between the modes located at the FP cavity

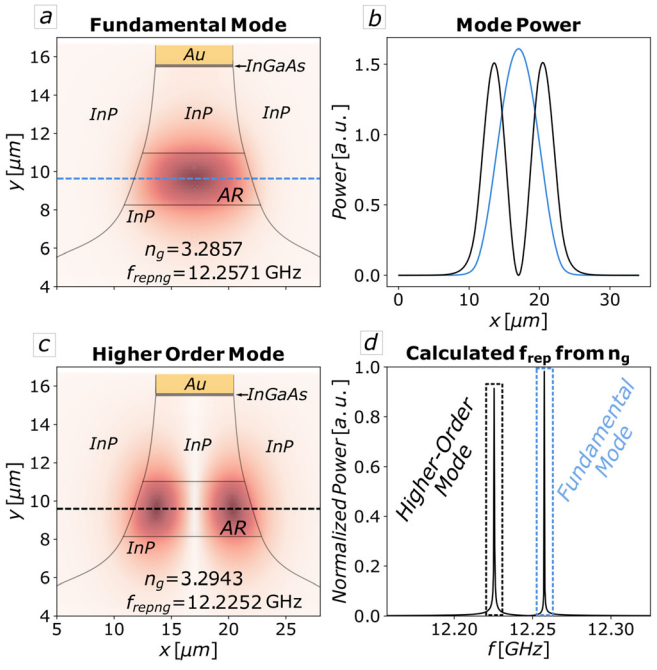


**FIG. 1.** Simulation results: (a) and (c) show the intensities of the simulated transverse modes overlapped with the QCL structure. The shape and dimensions of the active region after wet etching of the QCL are illustrated. The waveguide supports the fundamental mode, observed as a single lobe in the far-field, and a higher-order mode, observed as a dual-lobe far-field state. (d) Repetition frequencies calculated using the resulting group refractive $n_g$ index obtained from the mode solver tool with a frequency difference between the two repetition frequencies of several MHz. (b) Mode normalized power plotted along the red and blue lines indicated in (a) and (c).

round trip frequency that can be easily accessed in the RF domain. This is the so-called laser beatnote. In our case, the two separated beatnote frequencies associated with the two corresponding mode profiles lead to the assumption that RF-modulation at the correct frequency can be exploited to excite the fundamental mode in the cavity while suppressing higher-order modes. The suppression of higher-order transverse modes is proven to be advantageous for most applications. A Gaussian beam shape facilitates an increased overlap of the mode with the QCL's active region, increasing lasing efficiency. Furthermore, fundamental mode operation aids in increasing the focusing quality of optical components and, thus, simplifies simulation and design of more complex optical MIR systems.[28,29] The ideal beam characteristic would be represented by a diffraction-limited Gaussian beam-shape.[30] Given the importance of the far-field intensity characteristic, different concepts and approaches for higher-order mode suppression in high-power, broad-ridge waveguide QCLs have been investigated and demonstrated successfully in the past. Examples include tapered waveguide QCLs,[31] corrugated sidewalls in broad area devices,[32] integrated planar horn structures,[26] and the use of short trenches to create lateral constrictions in the waveguide[33] enabling high-power operation while maintaining the desired Gaussian-like single-lobe far-field characteristic. A downside to these methods, however, is the need for often complex processing techniques and specialized designs. In contrast, here we demonstrate an approach where any device optimized for RF-modulation can be adapted easily for high-power operation by just increasing the waveguide ridge width. The desired single-lobe far-field operation is achieved simply by injecting an RF signal at the repetition frequency of the fundamental transverse mode. We experimentally confirm our hypothesis by employing the setup illustrated in Fig. 2(a). In order to increase the efficiency of the RF injection, the QCL waveguide is comprised of two electrically separated top contacts: a longer gain section (mm range) and an additional short modulation section (300 $\mu$m). The QCL is mounted epi-side up on a copper submount and driven at a stabilized temperature of 16 °C. The short modulation section is contacted with an RF-probe [see Fig. 2(a)] and additional to the bias voltage, an RF-modulation signal is superimposed using a bias-Tee. To evaluate the far-field characteristic, a 200 MHz VIGO MCT photodetector is mounted on a rotational stage with the detector input located at a distance of 10 cm parallel to the front facet of the laser. The photodetector output voltage is monitored with a Keithley SMU for every step of the rotational stage over a radial range from −50° to +50° relative to the emission axis. An experimentally recorded dual-lobe far-field characteristic of the free-running QCL is shown in Fig. 2(b) for a gain section bias of 1250 mA. In order to determine the exact mode switching conditions, the detector remains parallel to the front facet of the laser [see inset on bottom right in Fig. 3(b)] corresponding to the minimum of the dual-lobe far-field state given in Fig. 2(a). As a first step, the position of the free-running QCL beatnote, which corresponds to the dual-lobe state from Fig. 2(b), is evaluated over the gain-section bias range of interest (1150–1350 mA). The recorded beatnote frequency varies from 12.214 GHz close to threshold (1150 mA) to 12.189 GHz close to roll-over (1350 mA) as shown in Fig. 3(a) and the LIV characteristic in the inset on the bottom left in Fig. 3(b) corresponding to a representative laser on the chip used for the far-field sweep. The DC-bias of the modulation section was set to 64 mA for all following measurements to ensure frequency comb operation of the QCL, evident from the

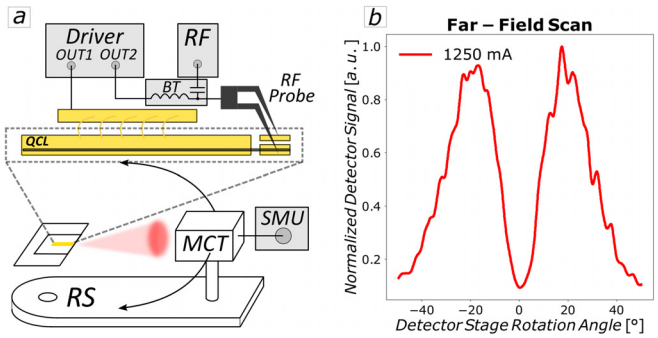


**FIG. 2.** Experimental setup: (a) THe two section FP-QCL is aligned onto a mercurium cadmium tellurite (MCT) detector mounted on a rotational stage (RS) for analysis of the far-field. The detectors DC output signal is monitored with a Keithley Sourcemeter Unit (SMU) while rotating the stage. The QCL waveguide consists of two electrically separated sections, a gain section and an RF-optimized modulation section. Both sections are biased independently and an RF signal can be injected additionally over a bias-tee (BT) into the modulation section. (b) Measurement of the dual-lobe far-field of the free-running QCL without modulation recorded with the setup given in (a).

stable and narrow beatnote signal over the entire gain section bias range. The second step consists of sweeping the frequency of the modulation signal over a range from 12 to 13 GHz around the free-running laser beatnote frequency for every increment of the QCL gain section bias. We show the MCT-PD output signal in Fig. 3(b), depending on the injected RF-modulation signal for each bias point. The inset on the top right illustrates the change in detector signal in dependence of the modulation frequency for one bias point along the white-dotted line. An increase in signal, thus, indicates a shift toward the single-lobe state in the far-field. We then use a peak-finding algorithm to find both the position of the free-running beatnote and the maximum of the PD signal under RF-injection indicating fundamental mode operation [red dots in the heatmaps of Figs. 3(a) and 3(b)] for every bias point. The difference between the frequency of the free-running beatnote and the evaluated RF-modulation frequency for single-lobe operation yields the mode switching frequency range. The range could be pinpointed to $60 \pm 3$ MHz above the free-running laser beatnote of the intrinsic dual-lobe state over the entire investigated lasing bias range. This result is in good correspondence with the simulation results predicting the repetition frequency for fundamental mode operation above the repetition frequency of the free-running QCL according to the group refractive index $n_g$ of the respective modes. Plot (c) in Fig. 3 shows the recorded far-fields of the investigated QCL for three different gain section bias points (1150, 1250, and 1350 mA). The black lines represent the far-field for the free-running laser. The intrinsic dual-lobe, higher-order transverse mode is evident for all three investigated bias points. Injecting an RF signal of intermediate strength (15 dBm modulation power, indicated with the green line) induces a transition state between the higher-order and fundamental transverse mode, already hinting that we are on the right path. Injecting a stronger signal (above 25 dBm depicted as red and blue lines) clearly shows the desired single-lobe behavior of the fundamental transverse mode. The dual-lobe state is successfully suppressed by the applied RF-modulation signal at the mode switching frequency. An extended study on wider ridges and also other types of lasers is ongoing. The main limitation of moving to even wider ridges is imposed by thermal dissipation, which makes it necessary to investigate broad lasers in epi-down configuration.

Another important metric used to characterize frequency combs and their viability for sensing applications is their coherence. For this purpose, we perform a Shifted Wave Interference Fourier Transform Spectroscopy (SWIFTS) measurement[34] of both the higher-order and

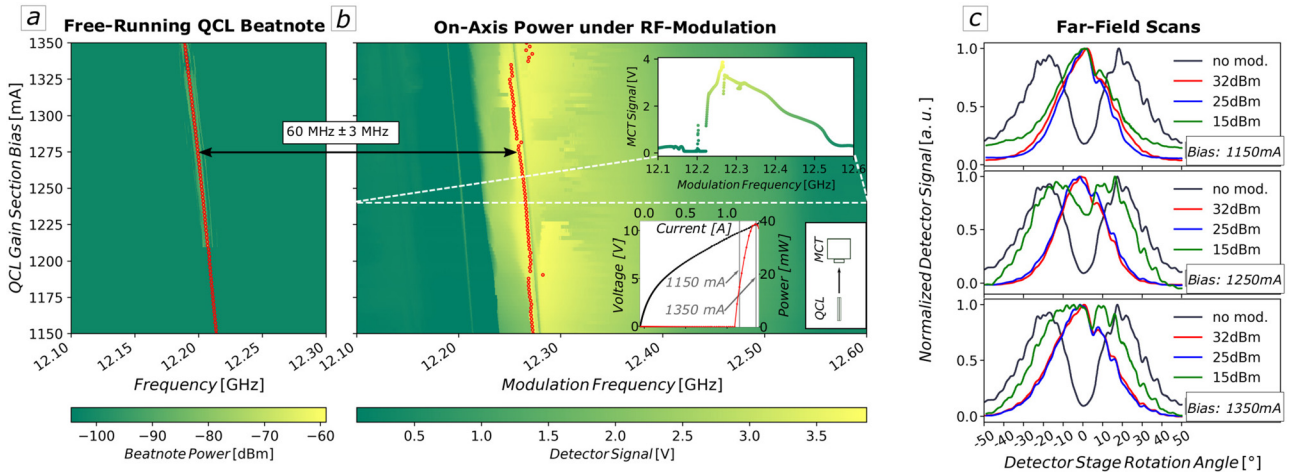


**FIG. 3.** Transverse mode switching condition: (a) heatmap of the free-running QCL beatnote recorded with a spectrum analyzer while sweeping the bias of the gain section. (b) Heatmap of the MCT-PD signal at the center position (see inset bottom right). The QCL gain section bias is swept from 1150 to 1350 mA corresponding to 50 mA above lasing threshold up to roll-over at 1350 mA (see LIV characteristic inset bottom left), while sweeping the modulation frequency from 12 to 13 GHz for every bias point. The red dots in (a) and (b) indicate the results of the peak finding algorithm. The frequency of the position of the free-running QCL beatnote is subtracted from the modulation frequency for maximum PD signal to obtain the mode switching frequency shown in the figure as $60 \pm 3$ MHz above the free-running beatnote. (c) Recorded far-fields over a range of $\pm 50°$ around the center of the emission axis for no modulation applied (higher order transverse mode) and three different modulation powers (transition to fundamental transverse mode) at three different gain bias points.

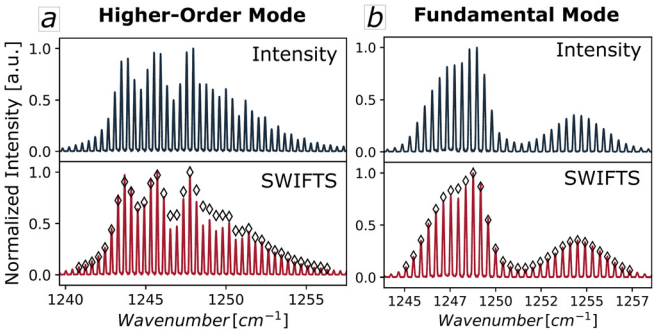


**FIG. 4.** SWIFTS measurement: (a) and (b) recorded intensity and reconstructed SWIFTS spectrum for the free-running QCL in the higher-order transverse mode state in (a) and the QCL under RF-modulation in the fundamental transverse mode and, thus, single-lobe far-field operation in (b). Coherent, low phase noise comb operation is given for both recorded states according to the shape and form of the reconstructed SWIFTS spectrum.

fundamental transverse mode induced by RF-modulation. Figures 4(a) and 4(b), therefore, show the recorded intensity spectrum and the reconstructed SWIFTS spectrum of the QCL for the free-running case (higher order transverse mode) in (a) and the case where RF-modulation in the mode switching frequency range was applied (fundamental transverse mode) in (b) for a gain section bias of 1250 mA and modulation power of 32 dBm. From the identical envelopes of both the intensity and SWIFTS spectra, one can infer that the QCL operates in the frequency comb regime. The coherence of the state, indicated by the stable equidistant comb modes, remains high after applying RF-modulation. Thus, the laser is forced to emit a single-lobe far-field, while retaining a high degree of coherence, both characteristics which are highly appealing for sensing applications.

In conclusion, we have presented a reliable technique to provide high-power broader ridge waveguide QCLs, which emit in the fundamental transverse mode state. The excitation of undesired higher-order transverse modes is eliminated by employing RF-modulation. The conditions for higher order mode suppression were evaluated with a straightforward technique. We demonstrate an excellent single-lobe far-field characteristic for modulation frequencies $60 \pm 3$ MHz above the free-running laser beatnote for modulation powers exceeding 25 dBm. Furthermore, we preserve coherently locked frequency comb operation of the laser under modulation, rendering this technique suitable for power scaling of semiconductor laser frequency combs.

## AUTHOR DECLARATIONS

### Conflict of Interest

The authors have no conflicts to disclose.

### Author Contributions

**Sandro Dal Cin:** Data curation (lead); Investigation (lead); Methodology (lead); Software (equal); Visualization (lead); Writing – original draft (lead); Writing – review and editing (lead). **Florian Pilat:** Conceptualization (supporting); Formal analysis (supporting); Resources (supporting). **Ales Konecny:** Software (equal); Visualization (supporting). **Nikola Opačak:** Supervision (supporting); Writing – original draft (supporting). **Gottfried Strasser:** Funding acquisition (equal); Project administration (equal). **Benedikt Schwarz:** Funding acquisition (equal); Project administration (equal); Writing – original draft (supporting); Writing – review and editing (supporting).

## DATA AVAILABILITY

The data that support the findings of this study are available from the corresponding author upon reasonable request.

## REFERENCES

[1]J. Faist, F. Capasso, D. L. Sivco, C. Sirtori, A. L. Hutchinson, and A. Y. Cho, Science **264**, 553 (1994).
[2]A. Hugi, G. Villares, S. Blaser, H. C. Liu, and J. Faist, Nature **492**, 229–233 (2012).
[3]M. Geiser, J. Klocke, M. Mangold, P. Allmendinger, A. Hugi, P. Jouy, B. Horvath, J. Faist, and T. Kottke, Biophys. J. **114**, 173a (2018).
[4]S. B. G. Villares, A. Hugi, and J. Faist, Nat Commun. **5**, 5192 (2014).
[5]N. Opačak, S. Dal Cin, J. Hillbrand, and B. Schwarz, Phys. Rev. Lett. **127**, 093902 (2021).
[6]B. Bernhardt, A. Ozawa, P. Jacquet, M. Jacquey, Y. Kobayashi, T. Udem, R. Holzwarth, G. Guelachvili, T. W. Hänsch, and N. Picqué, Nat. Photonics **4**, 55–57 (2010).
[7]T. Udem, J. Reichert, R. Holzwarth, and T. W. Hänsch, Phys. Rev. Lett. **82**, 3568 (1999).
[8]D. Kazakov, M. Piccardo, Y. Wang, P. Chevalier, T. S. Mansuripur, F. Xie, C. en Zah, K. Lascola, A. Belyanin, and F. Capasso, Nat. Photonics **11**, 789 (2017).
[9]M. Piccardo, B. Schwarz, D. Kazakov, M. Beiser, N. Opačak, Y. Wang, S. Jha, J. Hillbrand, M. Tamagnone, W. T. Chen, A. Y. Zhu, L. L. Columbo, A. Belyanin, and F. Capasso, Nature **582**, 360 (2020).
[10]B. Meng, M. Singleton, J. Hillbrand, M. Franckié, M. Beck, and J. Faist, Nat. Photonics **16**, 142 (2022).
[11]J. Hillbrand, A. M. Andrews, H. Detz, G. Strasser, and B. Schwarz, Nat. Photonics **13**, 101 (2019).
[12]J. Hillbrand, D. Auth, M. Piccardo, N. Opačak, E. Gornik, G. Strasser, F. Capasso, S. Breuer, and B. Schwarz, Phys. Rev. Lett. **124**, 023901 (2020).
[13]J. Hillbrand, N. Opačak, M. Piccardo, H. Schneider, G. Strasser, F. Capasso, and B. Schwarz, Nat. Commun. **11**, 5788 (2020).
[14]F. Wang, K. Maussang, S. Moumdji, R. Colombelli, J. R. Freeman, I. Kundu, L. Li, E. H. Linfield, A. G. Davies, J. Mangeney, J. Tignon, and S. S. Dhillon, Optica **2**, 944 (2015).
[15]D. G. Revin, M. Hemingway, Y. Wang, J. W. Cockburn, and A. Belyanin, Nat. Commun. **7**, 11440 (2016).
[16]M. Beiser, N. Opačak, J. Hillbrand, G. Strasser, and B. Schwarz, Opt. Lett. **46**, 3416 (2021).
[17]B. Schneider, F. Kapsalidis, M. Bertrand, M. Singleton, J. Hillbrand, M. Beck, and J. Faist, Laser Photonics Rev. **15**, 2100242 (2021).
[18]S. Slivken and M. Razeghi, Photonics **9**, 231 (2022).
[19]P. Jouy, J. M. Wolf, Y. Bidaux, P. Allmendinger, M. Mangold, M. Beck, and J. Faist, Appl. Phys. Lett. **111**, 141102 (2017).
[20]Q. Y. Lu, M. Razeghi, S. Slivken, N. Bandyopadhyay, Y. Bai, W. J. Zhou, M. Chen, D. Heydari, A. Haddadi, R. McClintock, M. Amanti, and C. Sirtori, Appl. Phys. Lett. **106**, 051105 (2015).
[21]B. G. Lee, J. Kansky, A. K. Goyal, C. Pflügl, L. Diehl, M. A. Belkin, A. Sanchez, and F. A. Capasso, Opt. Express **17**, 16216 (2009).
[22]P. Rauter and F. Capasso, Laser Photonics Rev. **9**, 452 (2015).
[23]W. Zhou, Q.-Y. Lu, D.-H. Wu, S. Slivken, and M. Razeghi, Opt. Express **27**, 15776 (2019).
[24]N. Yu, L. Diehl, E. Cubukcu, D. Bour, S. Corzine, G. Höfler, A. K. Wojcik, K. B. Crozier, A. Belyanin, and F. Capasso, Phys. Rev. Lett. **102**, 013901 (2009).
[25]S. Ferré, L. Jumpertz, M. Carras, R. Ferreira, and F. Grillot, Sci. Rep. **7**, 44284 (2017).
[26]F. Wang, I. Kundu, L. Chen, L. Li, E. H. Linfield, A. G. Davies, S. Moumdji, R. Colombelli, J. Mangeney, J. Tignon, and S. S. Dhillon, Opt. Express **24**, 2174 (2016).

[27]B. Röben, M. Wienold, L. Schrottke, and H. T. Grahn, AIP Adv. **6**, 065104 (2016).
[28]J. George, R. Seihgal, S. M. Oak, and S. C. Mehendale, Appl. Opt. **48**, 6202 (2009).
[29]A. E. Siegman, Appl. Opt. **32**, 5893 (1993).
[30]A. E. Siegman, Proc. SPIE **1868**, 2–12 (1993).
[31]L. Nähle, J. Semmel, W. Kaiser, S. Höfling, and A. Forchel, Appl. Phys. Lett. **91**, 181122 (2007).
[32]W. W. Bewley, C. L. Canedy, C. S. Kim, M. Kim, C. D. Merritt, J. Abell, I. Vurgaftman, and J. R. Meyer, Opt. Express **20**, 20894 (2012).
[33]R. Kaspi, S. Luong, C. Yang, C. Lu, T. C. Newell, and T. Bate, Appl. Phys. Lett. **109**, 211102 (2016).
[34]D. Burghoff, Y. Yang, D. J. Hayton, J.-R. Gao, J. L. Reno, and Q. Hu, Opt. Express **23**, 1190 (2015).